Bioorganic & Medicinal Chemistry Letters 20 (2010) 38–41

Contents lists available at ScienceDirect

Bioorganic & Medicinal Chemistry Letters

journal homepage: www.elsevier.com/locate/bmcl

3D QSAR studies on 3,4-dihydroquinazolines as T-type calcium channel blocker by comparative molecular similarity indices analysis (CoMSIA)

Jin Ah Jeong [a], Haelim Cho [b], Soo Yeon Jung [a], Han Byul Kang [a], Jin Yeong Park [a], Jungahn Kim [a], Dong Joon Choo [a], Jae Yeol Lee [a,*]

[a] Research Institute for Basic Sciences and Department of Chemistry, College of Sciences, Kyung Hee University, Seoul 130-701, Republic of Korea
[b] T&J Tech Inc., Kasan-Dong, Keumchun-Gu, Seoul 153-770, Republic of Korea

ARTICLE INFO

Article history:
Received 24 July 2009
Revised 7 October 2009
Accepted 12 November 2009
Available online 15 November 2009

Keywords:
CoMSIA
3D QSAR
T-Type calcium channel
3,4-Dihydroquinazoline

ABSTRACT

A comparative molecular similarity indices analysis (CoMSIA) of a set of 42 3,4-dihydroquinazolines have been performed to find out the pharmacophore elements for T-type calcium channel blocking activity. The most potent compound, **33** (**KYS05090**) was used to align the molecules. As a result, we obtained 3D QSAR model which provided good predictivity for the training set (q^2 = 0.642, r^2 = 0.874) and the test set (r^2_{pred} = 0.884). This model would guide the design of new chemical entities potentially having high potency.

Calcium channels are the primary route for translating electrical signals into the biochemical events underlying key processes such as neurotransmitter release, cell excitability, and gene expression.[1] Among calcium channels, T-type or low voltage activated (LVA) calcium channels are thought to contribute to neuronal excitability and also play crucial roles in the control of blood pressure.[2] Therefore, T-type calcium channels are important therapeutic targets for the treatment of epilepsy, neuropathic pain, and cardiovascular diseases such as hypertension and angina pectoris.[3] A T-type calcium channel blocker, mibefradil (IC_{50} = 1.34 ± 0.49 μM; Posicor™), has been used in treatment of hypertension and stable angina.[4] Shortly following its introduction, mibefradil was withdrawn from the US market in May 1998 because of potential harmful interactions with other drugs.[5] Since the withdrawal of mibefradil, efforts aimed at discovery of new T-type calcium channel blockers have intensified.[6] As a result of continuous structure–activity relationship study on 3,4-dihydroquinazoline series, we have recently discovered **KYS05090** (entry **33**) which is a very potent blocker (IC_{50} = 41 ± 1 nM) against T-type calcium channel and also is as potent as doxorubicin against some human cancer cells without acute toxicity (Fig. 1).[7,8] Based on the library of synthetic 3,4-dihydroquinazolines, in the present study, we have performed the 3D QSAR studies on these compounds by comparative molecular field similarity indices analysis (CoMSIA) method, which produces three-dimensional models to indicate the regions that affect biological activity with the change in chemical substitution.[9]

Among the library of 3,4-dihydroquinazoline compounds reported by our group, 42 compounds showing a wide range of IC_{50} values (0.041–35.8 μM) were selected for the present study. The biological activities (IC_{50} data) on HEK 293 cell with stabilized α_{1G} T-type calcium channel were converted to pIC_{50} ($-\log IC_{50}$) values and used for CoMSIA analysis. Thirty-five molecules were used as the training set and the remaining seven molecules were used as the test set to validate the developed CoMSIA model (Table 1). All molecular modeling calculations were performed using SYBYL8.1 on Linux.[10] Energy minimizations were performed using Tripos Force Field[10,11] and Gasteiger-Huckel charge with conjugate gradient method with convergence criterion of 0.05 kcal/mol. As no structural information is available about ligand–receptor complexes for T-type calcium channel, the minimum energy conformation of **33** (**KYS05090**: lowest IC_{50} value) via simulated annealing protocol (heating molecule at 700 K for 1000 fs and annealing molecule to 200 K for 1000 fs) was used as a template to align the selected compounds assuming that this template is a bioactive conformation.[12] In particular, this conformation was obtained based on arbitrary 4*S* configuration of **33** because all 3,4-dihydroquinazoline compounds were prepared as racemates and thus this arbitrary *S* configuration was used for all the molecules. We aligned the molecules using this template as shown in Figure 2.

The steric, electrostatic, and hydrophobic potential fields for CoMSIA were calculated at each lattice intersection of a regularly spaced grid of 2.0 Å and attenuation factor of 0.3. The regression

* Corresponding author. Tel.: +82 2 961 0726; fax +82 2 966 3701.
E-mail address: ljy@khu.ac.kr (J.Y. Lee).

0960-894X/$ - see front matter © 2009 Elsevier Ltd. All rights reserved.
doi:10.1016/j.bmcl.2009.11.049

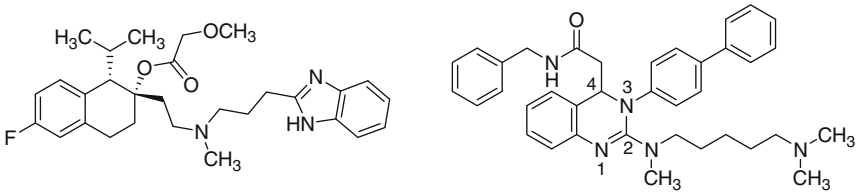

mibefradil KYS05090 (entry 33)

Figure 1. T-type calcium channel blockers.

Table 1
Structures, actual and predicted inhibitory activities of 3,4-dihydroquinazolines

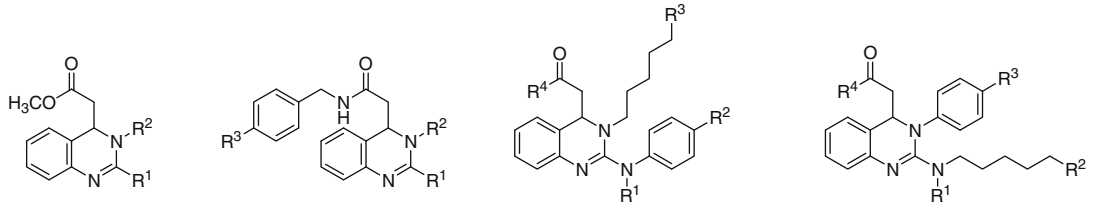

Type I (1-2) Type II (3-17, 36-37, 40) Type III (18-25) Type IV (26-35, 38-39, 41-42)

Entry	R_1	R_2	R_3	R_4	Actual pIC_{50}	Pred. pIC_{50}	Residual
Training set							
1	1-Piperidinyl	Ph	—	—	4.558	4.536	−0.022
2	Ph	Ph	—	—	4.971	4.978	0.008
3	4-Me-piperazinyl	Ph	H	—	4.446	4.638	0.192
4	1-Piperidinyl	Ph	NH_2	—	4.885	5.210	0.324
5	1-Piperidinyl	Ph	*p*-Me–Ph–SO_2NH	—	6.770	6.326	−0.444
6	$N(Me)_2$	Ph	NO_2	—	6.456	6.570	0.114
7	$N(Me)_2$	Ph	*p*-Me–Ph–SO_2NH	—	6.201	6.044	−0.157
8	$N(Me)_2$	Ph	*p*-F–Ph–SO_2NH	—	6.367	6.286	−0.081
9	1-Piperidinyl	Et	NO_2	—	6.061	5.920	−0.141
10	1-Piperidinyl	Et	*p*-Me–Ph–SO_2NH	—	6.018	5.953	−0.065
11	1-Piperidinyl	Et	*p*-F–Ph–SO_2NH	—	5.983	5.810	−0.173
12	$N(Me)_2$	Et	NO_2	—	5.664	5.989	0.325
13	$N(Me)_2$	Et	*p*-Me–Ph–SO_2NH	—	5.951	5.840	−0.111
14	$N(Me)_2$	Et	*p*-F–Ph–SO_2NH	—	5.387	5.715	0.328
15	1-Piperidinyl	Et	H	—	5.339	4.697	−0.642
16	$N(Me)_2$	Et	H	—	4.617	4.761	0.144
17	1-Piperidinyl	Ph	2-Thiophenyl–SO_2NH	—	5.996	6.011	0.015
18	H	Ph	NH_2	OCH_3	6.523	6.344	−0.179
19	H	Ph	NH–^{t}Boc	OCH_3	6.432	6.640	0.208
20	H	Ph	NH–^{t}Boc	$PhCH_2NH$	6.770	7.102	0.332
21	H	Ph	NH_2	$PhCH_2NH$	6.854	6.828	−0.026
22	H	H	NH_2	OCH_3	5.038	5.308	0.270
23	H	H	NH–^{t}Boc	OCH_3	5.644	5.587	−0.057
24	H	H	NH–^{t}Boc	$PhCH_2NH$	5.921	5.979	0.058
25	H	H	NH_2	$PhCH_2NH$	5.343	5.416	0.073
26	H	NH_2	Ph	OCH_3	6.252	6.453	0.201
27	Me	1-Pyrrodinyl	H	OCH_3	5.234	5.551	0.318
28	Me	1-Pyrrodinyl	H	$PhCH_2NH$	5.377	5.663	0.287
29	Me	1-Pyrrodinyl	Ph	$PhCH_2NH$	6.585	6.637	0.052
30	H	NH_2	H	OCH_3	5.735	5.488	−0.247
31	H	NH-^{t}Boc	H	OCH_3	5.695	5.559	−0.136
32	H	NH-^{t}Boc	H	$PhCH_2NH$	6.244	6.060	−0.184
33	Me	$N(Me)_2$	Ph	$PhCH_2NH$	7.384	6.606	−0.778
34	H	NH-^{t}Boc	Ph	$PhCH_2NH$	6.796	6.892	0.096
35	H	NH_2	Ph	$PhCH_2NH$	6.886	6.982	0.096
Test set							
36	1-Morpholinyl	Ph	H	—	4.666	4.558	−0.108
37	$N(Me)_2$	Et	NH_2	—	4.896	5.045	0.149
38	H	NH-^{t}Boc	Ph	OCH_3	6.168	6.428	0.261
39	H	NH_2	H	$PhCH_2NH$	5.505	5.754	0.250
40	1-Piperidinyl	Ph	NO_2		5.631	6.125	0.494
41	Me	1-Pyrrodinyl	Ph	OCH_3	6.469	6.521	0.052
42	Me	$N(ME)_2$	Ph	OCH_3	6.638	6.521	−0.118

IC_{50} values were measured by HEK 293 cell assay; Entry **33** = **KYS05090**.

analysis of the CoMSIA field energies was performed using PLS (partial least squares) with LOO (leave-one-out) cross-validation. The summary of the statistical results obtained for CoMSIA studies is shown in Table 2. We found that the CoMSIA hydrophobic

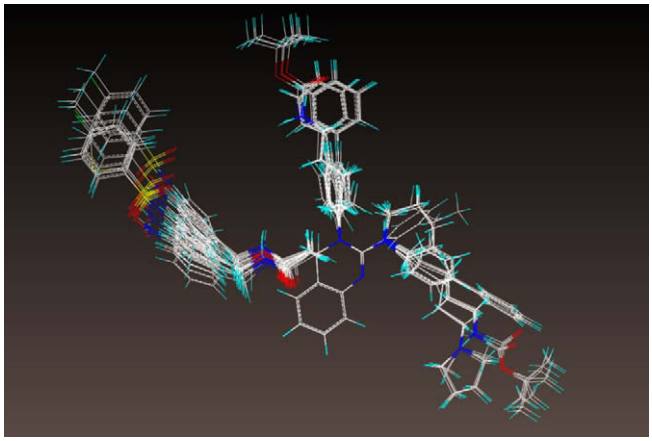

Figure 2. Alignment based on minimum energy conformation of **33** (**KYS05090**).

Table 2
The summary of PLS (partial least square) analyses

q^2	N	r^2	SEE	F	r^2_{pred}	Fraction		
						Steric	Electrostatic	Hydrophobic
0.642	3	0.874	0.274	71.518	0.884	0.283	0.249	0.468

q^2—Leave-one-out cross-validated correlation coefficient; N—optimum number of components; r^2—non-cross-validated correlation coefficient; SEE—standard error of estimate; F—F-test value; fraction—relative contributions of each CoMSIA descriptor.

Table 3
The summary of scrambling stability test

No. of components	Q^2	cSDEP	$dq^{2'}/dr^2yy'$
1	0.262	0.641	0.695
2	0.520	0.525	0.886
3	0.577	0.500	0.986
4	0.572	0.511	1.092
5	0.544	0.534	1.257

$Q^2 = 1 - (\text{cSDEP})^2$—the predictivity of the model after potential effects of redundancy have been removed, that is, the expected value of q^2 at the specified critical point; cSDEP—scaled cross-validated standard error (SDEP normalized by the standard deviation of the dependent variables); $dq^{2'}/dr^2yy'$—the slope of q^2 with respect to the correlation of the original dependent variables versus the perturbed dependent variables.

descriptor played a more significant role (46.8% of contribution) than descriptors such as steric (28.3%) and electrostatic (24.9%) in the prediction of biological activity. A good value of 0.874 for r^2 was obtained for this model with the q^2 of 0.642. To validate the predictive power of the model derived using the training set, biological activities of the test set molecules were predicted. The predictive ability of the model is expressed by the predictive r^2 value.

The scrambling stability test represents a second internal method to ensure the validity of 3D QSAR models.[13] QSAR models which are unstable (i.e., which change greatly with small changes in underlying response values) are characterized by slopes ($dq^{2'}/dr^2yy'$) greater than 1.20. Stable models (i.e., which change proportionally with small changes in underlying data) have slopes near unity. To investigate the risk of chance correlations, the potencies of the 35 compounds were randomly scrambled and the q^2 values were calculated using LOO cross-validation. Again, the scrambling stability test has to be repeated several times to avoid chance results. According to the results presented in Table 3, four cases (1, 2, 3, and 4-component models) showed the acceptable range values of $dq^{2'}/dr^2yy'$. Among them, 3-component model is most reliable because it showed the highest Q^2 value (0.577), the lowest cSDEP (0.500) and the nearest $dq^{2'}/dr^2yy'$ value to unity. It also coincides with the result of PLS analyses.

The contour maps (Fig. 3) produced by CoMSIA were analyzed by superimposing them onto **KYS05090** as this was the most active molecule of 3,4-dihydroquinazoline series.

With respect to steric contour plot (a) in Figure 3, three large green contours indicated the importance of the presence of bulky groups at C-2, C-3, and C-4 positions in 3,4-dihydroquinazoline skeleton for channel blocking activity. Thus, compounds **16 and 37** with less bulky groups at these regions exhibited the decreased activities compared to those of compounds **5**, **20**, **21**, **33** with three bulky groups. In general, compounds (Types II–IV) with a benzyl amide at C-4 position exhibited increased activities compared to those of compounds **1 and 2** (Type 1) with a methyl ester group. In particular, compound **5** with a 4-phenylsulfonamido-benzyl group at C-4 position exhibited the increased activities compared to that of compound **4** with a *p*-aminobenzyl amide group. In the case of Type III and Type IV series, finally, compounds **(18–21**, **26**, **38)** with a biphenyl group at C-2 or C-3 position generally exhibited increased activities compared to those of compounds **(22–25** and **30–31)** with a phenyl group. With respect to hydrophobic contour plot (b) in Figure 3, two large yellow contours indicated the importance of the presence of hydrophobic groups at C-2

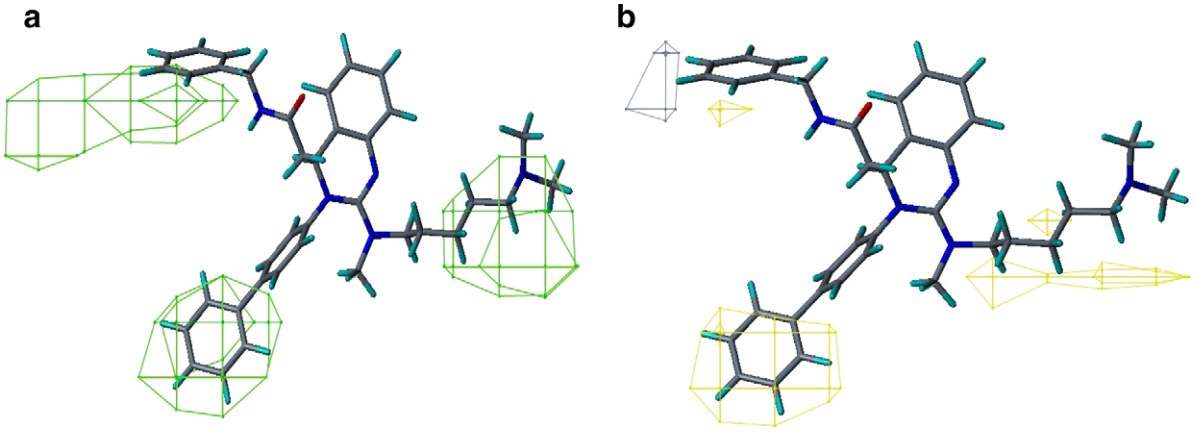

Figure 3. (a) CoMSIA steric contour plot with **33** (**KYS05090**): green contours indicate regions where the bulky group increases activity, whereas yellow contours indicate regions where the bulky group decreases activity although not shown here; (b) CoMSIA hydrophobic contour plot with **33**: yellow contours indicate regions where hydrophobic group increases activity, whereas gray contours indicate regions where hydrophobic group decreases activity.

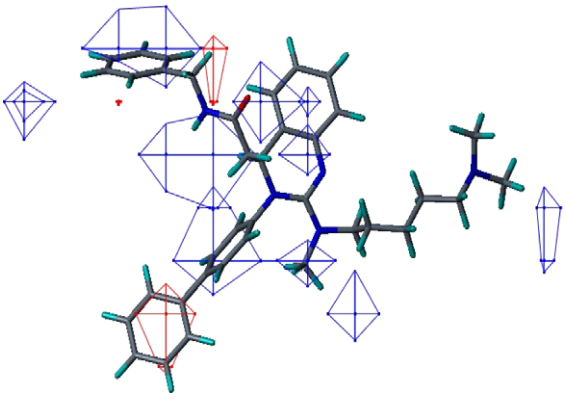

Figure 4. CoMSIA electrostatic contour plot with **33**: blue contours indicate regions where positive charge increases activity, whereas red contours indicate regions where negative charge increases activity.

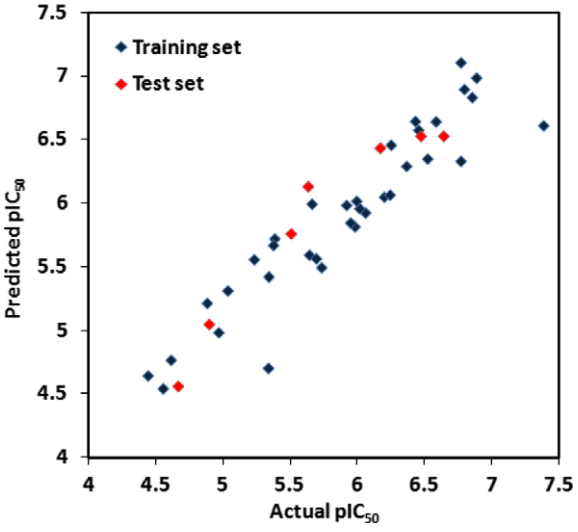

Figure 5. Actual versus predicted pIC_{50} of training and test set molecules.

and C-3 positions for channel blocking activity. Thus, compounds with a biphenyl group at C-2 or C-3 position in the case of Type III and Type IV series generally exhibited better activity than compounds with a phenyl group (**18**–**21** vs **22**–**25**; **26**, **29**, **38**, **33** vs **27**–**28**, **30**–**32**, **39**). Both steric and hydrophobic contour plots explained the strongest activity of **33** (**KYS05090**) in this series very well. CoMSIA electrostatic contour map showed that negative charge favored red regions are localized in the center area of biphenyl group at C-2 position and in the above area of amide nitrogen at C-4 as shown in Figure 4. Therefore, electrostatic plot also explained the best activity of **33** (**KYS05090**) in this series. In addition, this contour map reasoned the poor activities of compounds **3** and **36** in Type II series, which have a 4-methylpiperazine (nitrogen atom) and a morpholine (oxygen atom) in positive charge favored blue regions at C-2 position, respectively.

Figure 5 shows plots of actual versus predicted activities of training and test sets of CoMSIA. Blue diamond shows the predictions of the training set and red shows that of test set. The actual and predicted value of the training and test set molecules showed a linear relationship. The predictive r^2 value of the test set is 0.884.

In conclusion, CoMSIA studies on 42 3,4-dihydroquinazolines were carried out to develop a 3D QSAR model that provided good predictivity for the training set (q^2 = 0.642, r^2 = 0.874) and the test set (r^2_{pred} = 0.884). The resultant model can be extrapolated to predict novel and more potent molecules. CoMSIA 3D-maps obtained from the analysis can be used for the design of new chemical entities with high T-type calcium channel blocking activity.

Acknowledgment

This research was supported by Basic Science Research Program through the National Research Foundation of Korea (NRF) funded by the Ministry of Education, Science and Technology (2009-0088135).

References and notes

1. (a) Barclay, J. W.; Morgan, A.; Burgoyne, R. D. *Cell Calcium* **2005**, *38*, 343; (b) Zheng, X.; Bobich, J. A. *Brain Res. Bull.* **1998**, *47*, 117; (c) Himpens, B.; Missiaen, L.; Casteels, R. *J. Vasc. Res.* **1995**, *32*, 207; (d) Levi, A. J.; Brooksby, P.; Hancox, J. C. *Cardiovasc. Res.* **1993**, *27*, 1743.
2. (a) Opie, L. H.; Frishman, W. H.; Thadani, U. Calcium Channel Antagonists (Calcium Entry Blockers). In *Drugs for the Heart*; Opie, L. H., Ed., 4th ed.; WB Saunders: Philadelphia, 1994; p 50; (b) Abernethy, D. R.; Schwartz, J. B. N. *Engl. J. Med.* **1999**, *341*, 1447; (c) Thadani, U. *Curr. Opin. Cardiol.* **1999**, *14*, 349.
3. (a) Flatters, S. J. L. *Drugs Future* **2005**, *30*, 573; (b) Nelson, M. T.; Todorovic, S. M. *Curr. Pharm. Des.* **2006**, *12*, 2189; (c) Perez-Reyes, E. *Physiol. Rev.* **2003**, *83*, 117; (d) Vassort, G.; Alvarez, J. *J. Cardiovasc. Electrophysiol.* **1994**, *5*, 376.
4. (a) Clozel, J.; Ertel, E.; Ertel, S. *J. Hypertens.* **1997**, *15*, S17; (b) Hermsmeyer, K.; Mishra, S.; Miyagawa, K.; Minshall, R. *Clin. Ther.* **1997**, *19*, 18; Van der (c) Vring, J.; Cleophas, T.; Van der Wall, E.; Niemeyer, M. *Am. J. Ther.* **1999**, *6*, 229.
5. Asirvatham, S.; Sebastian, C.; Thadani, U. *Drug Safety* **1998**, *19*, 23.
6. (a) Park, J. H.; Choi, J. K.; Lee, E.; Lee, J. K.; Rhim, H.; Seo, S. H.; Kim, Y.; Doddareddy, M. R.; Pae, A. N.; Kang, J.; Roh, E. J. *Bioorg. Med. Chem.* **2007**, *15*, 1409; (b) Doddareddy, M. R.; Choo, H.; Cho, Y. S.; Rhim, H.; Koh, H. Y.; Lee, J.-H.; Jeong, S.-W.; Pae, A. N. *Bioorg. Med. Chem.* **2007**, *15*, 1091; (c) Jo, M. N.; Seo, H. J.; Kim, Y.; Seo, S. H.; Rhim, H.; Cho, Y. S.; Cha, J. H.; Koh, H. Y.; Choo, H.; Pae, A. N. *Bioorg. Med. Chem.* **2007**, *15*, 365; (d) Ku, I. W.; Cho, S.; Doddareddy, M. R.; Jang, M. S.; Keum, G.; Lee, J.-H.; Chung, B. Y.; Kim, Y.; Rhim, H.; Kang, S. B. *Bioorg. Med. Chem. Lett.* **2006**, *16*, 5244; (e) Furukawa, T.; Yamada, O.; Matsumoto, H.; Yamashita, T. WO2005051402, 2005.; (f) McCalmont, W. F.; Heady, T. N.; Patterson, J. R.; Lindenmuth, M. A.; Haverstick, D. M.; Gray, L. S.; MacDonald, T. L. *Bioorg. Med. Chem. Lett.* **2004**, *14*, 3691; (g) Jung, H. K.; Doddareddy, M. R.; Cha, J. H.; Rhim, H.; Cho, Y. S.; Koh, H. Y.; Jung, B. Y.; Pae, A. N. *Bioorg. Med. Chem.* **2004**, *12*, 3965; (h) Kumar, P. P.; Stotz, S. C.; Paramashivappa, R.; Beedle, A. M.; Zamponi, G. W.; Rao, A. S. *Mol. Pharmacol.* **2002**, *61*, 649.
7. Seo, H. N.; Choi, J. Y.; Choe, Y. J.; Kim, Y.; Rhim, H.; Lee, S. H.; Kim, J.; Joo, D. J.; Lee, J. Y. *Bioorg. Med. Chem. Lett.* **2007**, *17*, 5740.
8. Heo, J. H.; Seo, H. N.; Choe, Y. J.; Kim, S.; Oh, C. R.; Kim, Y. D.; Rhim, H.; Choo, D. J.; Kim, J.; Lee, J. Y. *Bioorg. Med. Chem. Lett.* **2008**, *18*, 4424.
9. (a) Klebe, G.; Abraham, U.; Meitzner, T. *J. Med. Chem.* **1994**, *37*, 4130; (b) Klebe, G.; Abraham, U. *J. Comput. Aided Mol. Des.* **1999**, *13*, 1; (c) Bohm, M.; Sturzebecher, J.; Klebe, G. *J. Med. Chem.* **1999**, *42*, 458.
10. SYBYL8.1. Tripos Inc., 1699 Hanley Road, St. Louis, MO 63144.
11. Clark, M.; Cramer, R. D., III; Van Opdenbosch, N. *J. Comput. Chem* **1989**, *10*, 982.
12. Crammer, R. D., III; Patterson, D. E.; Bunce, J. D. *J. Am. Chem. Soc.* **1988**, *110*, 5959.
13. Pick, A.; Müller, H.; Wiese, M. *Bioorg. Med. Chem.* **2008**, *16*, 8224.